Publications of the Astronomical Society of the Pacific
107: 179–183, 1995 February

Spectropolarimetry. II. Circular Polarization Optics and Techniques

ROBERT W. GOODRICH,[1] MARSHALL H. COHEN, AND ANGELA PUTNEY

Palomar Observatory, California Institute of Technology, Pasadena, California 91125
Electronic mail: goodrich@stsci.edu, mhc@astro.caltech.edu, axp@astro.caltech.edu

Received 1994 July 13; accepted 1994 November 18

ABSTRACT. We discuss the design of a Pancharatnam "superachromatic" quarter-wave plate and its application in two circular spectropolarimeters. The alignment and calibration of the polarimetry optics is discussed, as well as the data reduction techniques. In particular, the differences between reducing linear-polarimetry data and reducing circular polarimetry are emphasized.

1. INTRODUCTION

The recent marriage of high-efficiency CCD-based spectrographs and efficient polarization optics has allowed astronomers to open new avenues of research in a variety of fields. There are many spectropolarimeters in current use; see Coyne et al. (1988) for descriptions of several.

Most of these spectropolarimeters measure linear polarization, which is produced by reflection, synchrotron, and cyclotron emission, and dichroic absorption by dust grains in the interstellar medium. Paper I (Goodrich 1991) discussed the design and application of two such instruments. Circular spectropolarimetry, on the other hand, has not been explored as extensively. Circular polarization is produced in magnetic white dwarfs in both the continuum and absorption lines, and circular polarization in absorption lines split by the Zeeman effect is seen in the lower magnetic fields of magnetic Ap stars and other stars. Transmission through birefringent dust can also cause slight (tenths of a percent) circular polarization. Schmidt et al. (1986) used circular spectropolarimetry to study magnetic white dwarfs with the instrument described by Miller et al. (1980). During a hiatus of some years, little work on circular spectropolarimetry was published, Johnstone and Penston's (1986) work on T Tauri stars being one of the exceptions. Recently, the development of new, more efficient instruments has sparked renewed interest in circular polarimetry; see Mathys (1991), Schmidt et al. (1992), Cohen et al. (1993), Semel et al. (1993), and Valtaoja et al. (1993) for recent examples. Few papers in the literature, however, discuss the techniques for calibration and reduction which are peculiar to circular spectropolarimetry.

This paper discusses the design of a circular spectropolarimeter, followed by the data-taking, calibration, and reduction techniques. Much of the discussion draws heavily on results from Paper I, and the present work will only summarize most of this. The context is the circular spectropolarimeter retrofitted to the Double Spectrograph on the Palomar 5-m reflector, and a new linear/circular imaging spectropolarimeter we have built for the Keck telescope.

2. DESIGN

The quarter-wave plates used are of the Pancharatnam design, described in Paper I and originally by Pancharatnam (1955). Briefly, the general design uses two outer wave plates of the same retardance, τ_0, and orientation, with a third, inner, wave plate of retardance τ_1 and rotated by θ_P. The design discussed in Paper I uses three achromatic half-wave plates ($\tau_0=\tau_1=180°$) with the middle plate oriented at $\theta_P=58\overset{\circ}{.}7$, to produce a "super-achromatic" half-wave plate.[2] Another half-wave design uses $\tau_0=90°$, $\tau_1=360°$, and $\theta_P=58\overset{\circ}{.}7$. A characteristic of the Pancharatnam design is that the equivalent fast axis of the final wave plate varies with wavelength. As discussed in Paper I, for linear photometry this leads simply to a rotation of the (Q,U) coordinate system, with no loss in efficiency at measuring polarization. However, as Sec. 3 below will discuss, an error in position angle of the quarter-wave plate, or equivalently a drift in fast axis p.a. with wavelength, leads to a drop in the efficiency with which we measure circular polarization.

The design of a Pancharatnam quarter-wave plate is not so intuitive. One could produce a design which minimizes the maximum deviation from $\tau=90°$, but this produces large ($>10°$) drifts in the fast axis. As pointed out above, this decreases the efficiency of the wave plate. A better method is to maximize the minimum efficiency, which will be given in Sec. 3 as $\eta=\sin\tau\sin 2\theta$, where τ is the retardance of the Pancharatnam wave plate, and θ is the angle of the fast axis. To maximize this efficiency requires four free parameters; τ_0, τ_1, and θ_P described above, plus an arbitrary p.a. zero-point, which defines how the wave plate should be oriented with respect to the analyzer. The surface of best fit in this scheme is one with many local minima, although with some care it is easy to converge on a solution which has a very high efficiency across the entire design wavelength range of 3200 Å to 1.2 μm. Such a design is $(\tau_0, \tau_1, \theta_P, \theta_0)=(116\overset{\circ}{.}39, 180\overset{\circ}{.}77, 70\overset{\circ}{.}30, 30\overset{\circ}{.}47)$, which has a maximum retardance error of $3\overset{\circ}{.}87$, a maximum p.a. drift of $0\overset{\circ}{.}77$, and a minimum polarization efficiency of 99.75%. This design is presented in Fig. 1, which also shows the retardance of a single quartz MgF_2 quarter-wave "achromat".

In the Palomar Double Spectrograph (DBSP) we use a polymer quarter-wave plate made by Meadowlark Optics. This design, while less expensive, is not achromatic over as wide a wavelength range as the quartz/MgF_2 wave plates. In

[1]Current address: Space Telescope Science Institute, 3700 San Martin Drive, Baltimore, MD 21218.

[2]Note that we are defining a half-wave as defined by the design of a MgF_2/quartz achromatic half-wave plate in Paper I. Such a plate has a retardance of exactly a half-wave at two wavelengths, in this case 3500 and 7300 Å.

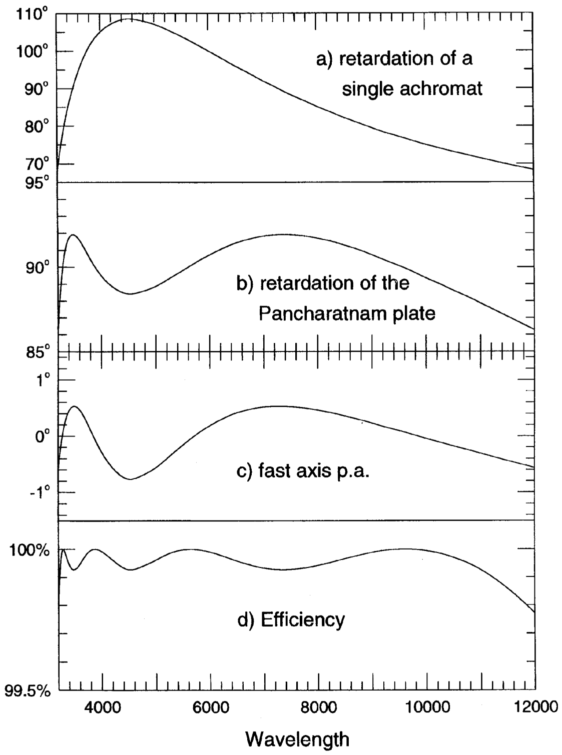

FIG. 1—The theoretical performance of a Pancharatnam quarter-wave plate design found by searching for global maxima of the minimum efficiency between 3200 Å and 1.2 μm. Plotted from top to bottom are: (a) the retardance of a single MgF_2/quartz achromatic quarter-wave plate, (b) the retardance of the Pancharatnam design, (c) the rotation of the equivalent fast axis of the Pancharatnam design, and (d) the overall efficiency of the design as described in the text.

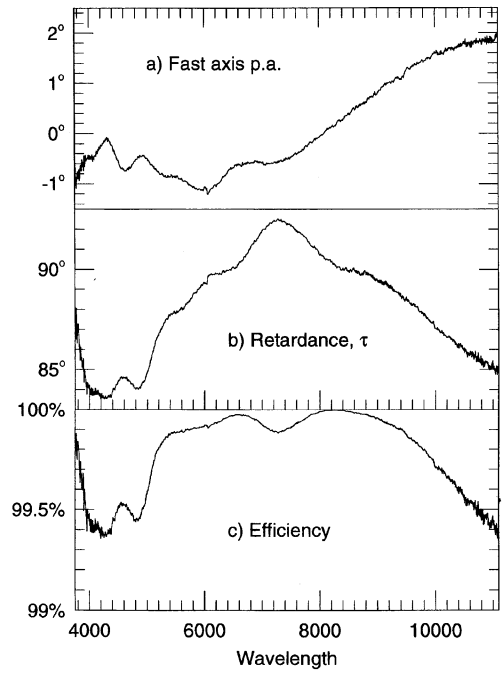

FIG. 2—The measured performance of the Keck quarter-wave plate. Note that while the efficiency of the design is not as great as the design in Fig. 1, it is still quite good.

the polarimeter being built for the Low-Resolution Imaging Spectrograph (LRIS; Oke et al. 1994) for the Keck telescope, we will use a quartz/MgF_2 superachromatic quarter-wave plate from B. Halle. Figure 2 shows the measured performance of the Keck quarter-wave plate. While the overall efficiency is less than the theoretical design described above, it is still good, $\geqslant$99.4% at almost all wavelengths measured.

The polarizing beamsplitter is a modified Glan-Taylor prism as described in Paper I. This prism has a length-to-depth ratio, *L/D*, of 1.034, but requires extra optics to compensate for the difference in optical path length between the two orthogonally polarized output beams.[3] Different schemes are discussed in Paper I, but an important conclusion is that any highly curved lens used to compensate for the different foci in the two beams also shifts the pupil position and introduces vignetting. Planar surfaces apparently do not introduce much if any vignetting, a fact confirmed at McDonald Observatory, where the use of a single block of fused silica is being used in a new imaging spectropolarimeter to do the focus compensation (Trammell and Hill 1993). Unfortunately, this increases *L/D* to 3.24 for a quartz block (2.63 for sapphire, with its higher refractive index), a value too large to be efficient when retrofitting polarimetry optics to many spectrographs.

In the Keck design, shown in Fig. 3, a block under the e ray folds that beam and provides focus compensation by sending the e ray sideways for some distance. To do this we use an internal reflection in a glass of appropriately high index of refraction. The reflection must be off a 45° face, since a smaller angle will cause the beam to hit the edges of the calcite beamsplitter before it can be straightened, and larger angles rapidly increase *L/D*. To reflect the extreme rays of an $f/16$ input beam wave we require a refractive index $n > 1.46$. To achieve high throughput in the UV we use Ultran-30, which has $n = 1.57 - 1.54$ throughout our de-

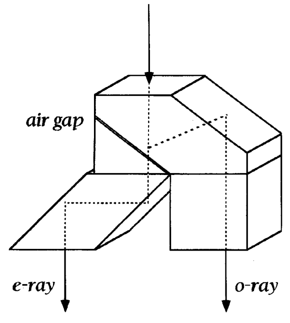

FIG. 3—A schematic diagram of the new beamsplitter, based on the design from Paper I. Focus compensation is accomplished using plane-parallel surfaces to avoid the problems of using highly curved lenses as in previous designs. A drawback of the design is the high *L/D* ratio of 2.034, translating into a more restricted field of view at the slit.

[3]Here, *L* is the size of the input face, not the overall size of the splitter, and *D* is the overall depth (the size of the beamsplitter along the spectrograph's light path); this ratio was called *L/W* in Paper I.

sign range, 3200 Å to 1.1 μm. To conserve space, under the o ray another block (also Ultran-30, although fused silica could be used as well) provides the remainder of the focus compensation by slowing the divergence of this beam. Note that without the o-ray block we could achieve the same end by making the horizontal path of the e ray longer. Adjusting the e-ray block's horizontal dimension optimizes the focus compensation. An additional feature of this design is that the focal plane is nearly unchanged from the spectrograph *without* the beamsplitter—divergence during the sideways motion compensates for the slower divergence within the calcite and Ultran-30. Figure 4 shows the calculated focus shift of both beams as a function of wavelength. This feature can be important for spectrographs with limited focus travel; the LRIS collimater, for example, has *no* focus capability. Again, though, it represents a compromise with the usable slit length (which will be $l=25$ mm, 25 arcsec with the LRIS), since $L/D=2.034$ with the Keck design.

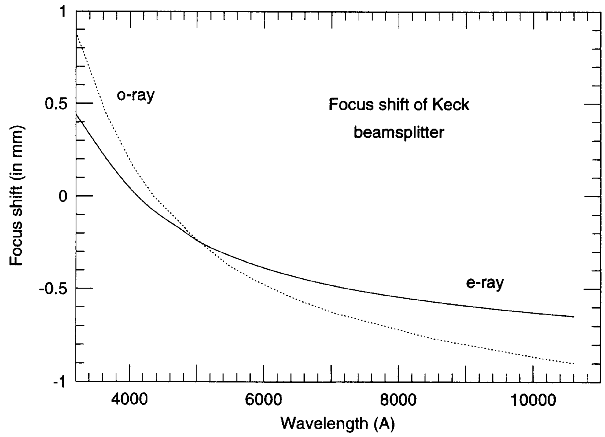

FIG. 4—The focus shift (at the slit) as a function of wavelength for both beams of the beamsplitter design shown in Fig. 3. A focus shift of 1 mm at the slit would cause a beam spreading of 10 μm on the detector of the LRIS. Note that the focus difference between the two beams is relatively small, as is the overall shift (from the spectrograph without the beamsplitter).

3. DATA-TAKING AND ANALYSIS

Much of the data-taking is done in a manner similar to that used to measure linear polarization using a half-wave plate. The reader is referred to Paper I for details. There are some important differences, however. To measure V with the DBSP we replace the half-wave plate with the quarter-wave plate; this technique will also be available at Keck. Two exposures are made, one with the mean fast axis of the wave plate at $\theta_1=45°$ to the beamsplitter axes, the other 90° from the first ($\theta_2=\theta_1+90°$). Following the analysis in Paper I, we measure two spectra at θ_1 and θ_2, respectively, and form the ratio

$$\frac{V''}{I''}=\frac{I''(\theta_2)-I''(\theta_1)}{I''(\theta_2)+I''(\theta_1)} \tag{1a}$$

$$=\frac{V\sin 2\theta_1 \sin\tau}{I+(\cos^2 2\theta_1+\sin^2 2\theta_1 \cos\tau)Q+\sin 2\theta_1 \cos 2\theta_1(1-\cos\tau)U}. \tag{1b}$$

Note that the most efficient use of a quarter-wave plate ($\tau=90°$) measuring V is to have $\theta_1=45°$, in which case $V''/I''=V/I$. Because the wave plate is not perfect, $\tau\neq 90°$ at most wavelengths. We assume that $\tau(\lambda)=90°+\Delta\tau(\lambda)$, with $\Delta\tau$ small, and define an efficiency $\eta_\tau=\cos\Delta\tau(\lambda)$. Also, since the fast axis of the wave plate rotates with wavelength, and we cannot perfectly align the wave plate's fast axis with the beamsplitter axes, we write $\theta_1(\lambda)=45°+\Delta\theta(\lambda)$. Accurate mechanical rotation assures that $\theta_2(\lambda)=\theta_1(\lambda)+90°$, however. In this case, because the functional form of the equation is so simple, we can correct for the two terms in the numerator precisely. We can also correct for the two terms in the denominator if we have some independent knowledge of Q and U. Note that in Paper I we saw that an error in $\theta_1(\Delta\theta\neq 0)$ resulted in a simple rotation of the (Q,U) coordinate system, with no loss in efficiency. In measuring V, however, the equation above indicates that $\Delta\theta\neq 0$ implies a loss in efficiency, $\eta_\theta=\cos 2\Delta\theta(\lambda)$. Quarter-wave plate designs hence should maximize the overall efficiency defined by $\eta=\cos 2\Delta\theta(\lambda)\cos\Delta\tau(\lambda)$, as described in Sec. 2. For the Halle wave plate in Fig. 2, $\eta\geqslant 99.4\%$, and theoretically this can be brought yet higher.

Note that the equations given above and in Paper I can in principle be algebraically solved so that, with some appropriate choice of wave-plate angles, a quarter-wave plate alone can be used to determine all four Stokes parameters, I, Q, U, and V. However, even though the equations may be solved algebraically, these techniques are generally unstable when used to try to determine Q and U. Care must be taken to check that any proposed observation and reduction techniques are robust against uncertainties in the wave-plate retardance and orientation, as well as noise in the spectra.

The second technique for measuring V, which may be implemented with the Keck polarimeter, is to place a stationary quarter-wave plate in the calibration wheel above the rotatable half-wave plate. Circularly polarized light becomes linearly polarized on passing through the quarter-wave plate, and the half-wave plate analyzes this linear polarization. If the fast axis of the quarter-wave plate is 45° to the axis of the beamsplitter, "cross talk" from linear polarization in the incident beam is minimized. Incident Q light is turned into circular polarization, and incident U light will keep its polarization; both of these are treated the same as unpolarized light by the rotating half-wave plate, which is oriented parallel and 45° to the beamsplitter axis to analyze the polarization. Numerical simulations show that this procedure works well when V is larger than the linear polarization, Q and U, but small errors in the retardances and orientations of the wave plates can produce significant errors in V if the linear polarization is large.

An approximate analytic solution for this "dual-wave plate" method allows us to apply first- or higher-order corrections to the measured circular polarization. V is estimated by observing with the half-wave plate at 0° and 45° relative to the beamsplitter axes, and calculating

$$\frac{V''}{I''}=\frac{I''(\theta)-I''(\theta+45°)}{I''(\theta)+I''(\theta+45°)}. \quad (2)$$

The full equation for V''/I'' in terms of the parameters of both wave plates is rather involved, so we present three simplified results. In the following discussion the subscripts q and h represent the quarter-wave plate and the half-wave plate, respectively. First, assuming pure circular polarization ($Q=U=0$) and exact retardances ($\Delta\tau_q=\Delta\tau_h=0$), Eq. (2) reduces to

$$\frac{V''}{I''}=\frac{V}{I}\cos(4\Delta\theta_h-2\Delta\theta_q), \quad (3)$$

indicating the efficiency loss due to misalignment of the plates and rotations of their fast axes. Second, again assuming $Q=U=0$, we assume that the fast axes are both accurately oriented ($\Delta\theta_q=\Delta\theta_h=0$) but the retardances are $\tau_q=90°+\Delta\tau_q$ and $\tau_h=180°+\Delta\tau_h$. Then

$$\frac{V''}{I''}=V\frac{\cos\Delta\tau_q+\cos(\Delta\tau_q+\Delta\tau_h)}{2I+V[\cos\Delta\tau_q-\cos(\Delta\tau_q+\Delta\tau_h)]}. \quad (4)$$

Finally, we relax all assumptions and linearize the equation in terms of $\Delta\theta$ and $\Delta\tau$ (Q and U are arbitrary here):

$$\frac{V''}{I''}\approx(V+\Delta\tau_qQ+\tfrac{1}{2}\Delta\tau_hQ(1+V)+(2\Delta\theta_q-4\Delta\theta_h)U)/I, \quad (5)$$

where $\Delta\tau$ and $\Delta\theta$ are in radians. With independent knowledge of Q and U we can use this equation to correct the measured V''/I'' for known imperfections in the wave plates. This dual-wave plate technique allows the Keck instrument to be rapidly switched between linear and circular polarimetry by simply rotating the quarter-wave plate out of the way. This ability is important for time-varying sources such as rotating magnetic white dwarfs.

4. ALIGNMENT AND CALIBRATION

As is clear from the discussion above, accurate alignment of the quarter-wave plate is important. In this context, "alignment" means assuring that the fast axis of the wave plate is at 45° to the axis of the polarizing beamsplitter. To align and calibrate a quarter-wave plate we would ideally like an efficient, broadband circular polarizer, analogous to sheet Polaroid and other broadband linear polarizers. Unfortunately, such a circular polarizer does not exist, except in forms such as linear Polaroids plus Fresnel rhombs which are as complex and require as much calibration of their own as do the wave plates. Hence we use a linear polarizer alone, placed at a known angle to the beamsplitter's fast axis. Since in the Pancharatnam design the wave plate's fast axis rotates with wavelength, we choose a wavelength at which the fast axis is near the mid-point of its range, or even better, the angle at which maximum overall efficiency is attained (Sec. 2). Then, without any wave plates, we place a piece of linear polarizer in a rotatable cell above the wave plate position. Attached to the cell is a mirror, which acts as an optical lever to reflect the beam from a laser pointer to a sheet of graph paper. The beam position can be read from the paper to provide an estimate of the angle of the wave plate. The polarizer is then rotated until one of the beams output by the beamsplitter is "nulled," i.e., minimized in intensity. The wave plate is then placed beneath the polarizer, its fast axis roughly aligned, and the same beam is nulled by rotating the wave plate, with the polarizer held stationary. The wave plate's fast axis is hence accurately parallel to the beam splitter's. We have found an accuracy of ~0°25 or better in performing this alignment, traceable largely to not having a precision rotation stage for the polarizer. However, this accuracy is quite adequate for a quarter-wave plate with a 3°–4° drift in the fast axis and with care higher accuracy can be achieved. The wave plate is then rotated by 45° to place it in its operating position. The half-wave plate can be aligned in the same way, if desired.

Calibration can be performed in a similar manner; a linear polarizer placed above the wave plate can be used to deduce $\Delta\theta(\lambda)$ and $\Delta\tau(\lambda)$ from the equations given in Sec. 3. Other, more general calibrations are described in Paper I.

5. DATA REDUCTION AND EXAMPLES

As discussed in Miller et al. (1988)[4] and Paper I, we take two observations, A and B, to measure a single Stokes parameter. Seeing, guiding, and transparency effects are removed by calculating the "balance factor," ω, and then the estimate

$$\frac{V''}{I''}=\frac{A-\omega B}{A+\omega B}. \quad (6)$$

If necessary, we then correct for $\Delta\theta(\lambda)$ and $\Delta\tau(\lambda)$, using the equations in Sec. 3. If we have independent estimates of $Q(\lambda)$ and $U(\lambda)$ we can also correct for the crosstalk, the leaking of linearly polarized light into the circular measurement. Note that some types of retarders, such as Pockels cells, may require more corrections than the first-order terms given in Eq. (5), if this dual wave-plate technique is being used.

An example of data we have collected with the Palomar spectropolarimeter is shown in Fig. 5. The magnetic white dwarf G 99−47 shows three components to the Hα absorption line in the total flux spectrum, indicating a polar magnetic-field strength of ~25 MG (Liebert et al. 1975). While the Hα absorption features are rather subtle in F_λ, the two circularly polarized σ components are quite striking in

[4]Note that in MRG 88 we advocated smoothing of the "balance factor" ω, in order to decrease the pixel-to-pixel noise in the final Stokes parameter. Tests and analytical work have shown that, while the noise in total flux, I, is decreased, the noise in the Stokes parameters Q, U, and V is not.

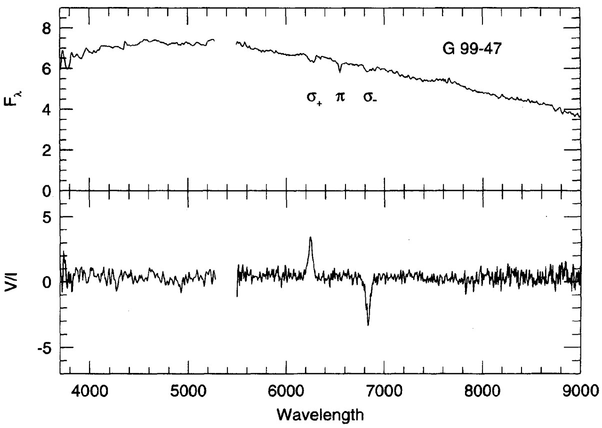

FIG. 5—An example of circular spectropolarimetry obtained with the double spectrograph on the Palomar 5-m telescope. The 14th magnitude white dwarf G 99−47 was observed for 12 minutes in each of two wave-plate positions, from which the total intensity, I, and the normalized circular polarization, V/I, were calculated. Note the Zeeman-shifted Hα σ components near 6240 and 6835 Å. While they are rather subtle in I, they stand out sharply in V/I.

$V(\lambda)/I(\lambda)$, at 6240 and 6835 Å (Fig. 5). A hint of the Hβ σ components is also seen, at 4630 and 4920 Å, although no Hβ absorption features are discernible in F_λ. The continuum V/I is also significant, 0.35%. Another example of data from the Palomar instrument is given in Cohen et al. (1993), which discusses observations of G 227-35.

We have described the techniques which we currently use to explore the circular polarization of astronomical sources. Unlike linear polarimetry, circular polarimetry requires more complicated alignment and calibration of the optics. The application of these techniques using present and future instruments will allow insight into many of the phenomena that produce circular polarization.

We would like to acknowledge Professor George R. Rossman for the use of his lab to test and characterize some of the polarimetry optics, and Earle Emery and Walter Schaal for their excellent engineering work on the Palomar and Keck systems, respectively. We also thank the referee, John Landstreet, for his useful suggestions.

REFERENCES

Cohen, M. H., Putney, A., and Goodrich, R. W. 1993, ApJ, 405, L67

Coyne, G. V., Magalhães, A. M., Moffat, A. F. J., Schulte-Ladbeck, R. E., Tapia, S., and Wickramasinghe, D. T. 1988, Polarized Radiation of Circumstellar Origin (Vatican City State, Vatican Observatory)

Goodrich, R. W. 1991, PASP, 103, 1314 (Paper I)

Johnstone, R. M. and Penston, M. V. 1986, MNRAS, 219, 927

Liebert, J., Angel, J. R. P., and Landstreet, J. D. 1975, ApJ, 202, L139

Mathys, G. 1991, A&AS, 89, 121

Miller, J. S., Robinson, L. B., and Goodrich, R. W. 1988, in Instrumentation for Ground-Based Astronomy, ed. L. B. Robinson (New York, Springer), p. 157 (MRG88)

Miller, J. S., Robinson, L. B., and Schmidt, G. D. 1980, PASP, 92, 702

Oke, J. B. et al. 1994, PASP, submitted

Pancharatnam, S. 1955, Proc. Indian Acad. Sci., A41, 137

Schmidt, G. D., Stockman, H. S., and Grandi, S. A. 1986, ApJ, 300, 804

Schmidt, G. D., Stockman, H. S., and Smith, P. S. 1992, ApJ, 398, L57

Semel, M., Donati, J.-F., and Rees, D. E. 1993, A&A, 278, 231

Trammell, S. R. and Hill, G. J. 1993, private communication

Valtaoja, L., Karttunen, H., Valtaoja, E., Shakhovskoy, N. M., and Efimov, Yu. S. 1993, A&A, 273, 393